Endocrine (2012) 41:236–247
DOI 10.1007/s12020-011-9555-1

ORIGINAL ARTICLE

Early protective effect of mitofusion 2 overexpression in STZ-induced diabetic rat kidney

Wan Xin Tang · Wei Hua Wu · Xiao Xi Zeng · Hong Bo · Song Min Huang

Received: 22 July 2011 / Accepted: 27 October 2011 / Published online: 18 November 2011

Abstract Diabetic nephropathy (DN) is a serious complication of diabetes with a poorly defined etiology and limited treatment options. Early intervention is key to preventing the progression of DN. Mitofusin 2 (Mfn2) regulates mitochondrial morphology and signaling, and is involved in the pathogenesis of numerous diseases. Furthermore, Mfn2 is also closely associated with the development of diabetes, but its functional roles in the diabetic kidney remain unknown. This study investigated the effect of Mfn2 at an early stage of DN. Mfn2 was overexpressed by adenovirus-mediated gene transfer in streptozotocin-induced diabetic rats. Clinical parameters (proteinuria, albumin/creatinine ratio), pathological changes, ultra-microstructural changes in nephrons, expression of collagen IV and phosph-p38, ROS production, mitochondrial function, and apoptosis were evaluated and compared with diabetic rats expressing control levels of Mfn2. Endogenous Mfn2 expression decreased with time in DN. Compared to the blank transfection control group, overexpression of Mfn2 decreased kidney weight relative to body weight, reduced proteinuria and ACR, and improved pathological changes typical of the diabetic kidney, like enlargement of glomeruli, accumulation of ECM, and thickening of the basement membrane. In addition, Mfn2 overexpression inhibited activation of p38, and the accumulation of ROS; prevented mitochondrial dysfunction; and reduced the synthesis of collagen IV, but did not affect apoptosis of kidney cells. This study demonstrates that Mfn2 overexpression can attenuate pathological changes in the kidneys of diabetic rats. Further studies are needed to clarify the underlying mechanism of this protective function. Mfn2 might be a potential therapeutic target for the treatment of early stage DN.

Keywords Diabetes · Kidney · Mitofusin 2 · Mitochondria · Collagen IV · MAPK

W. X. Tang (✉) · W. H. Wu · X. X. Zeng · H. Bo · S. M. Huang
Division of Nephrology, West China Hospital of Sichuan University, Chengdu, Sichuan, China
e-mail: kidney123@163.com

Introduction

Diabetic nephropathy (DN) is the leading cause of end-stage renal disease (ESRD) and a common but serious complication of diabetes. The pathologic features of early DN include mesangial cell proliferation, mesangial extracellular matrix (ECM) accumulation, glomerular basement membrane (GBM) thickening, and glomerular hypertrophy, which are followed eventually by diffuse nodular glomerulosclerosis [1]. Various mechanisms are implicated in the pathogenesis of DN, including increased aldose reductase activity [2], enhanced activity of protein kinase C isoforms [3], increased formation of advanced glycation end-products [4], hyperglycemia-driven mitochondrial overproduction of reactive oxygen species (ROS) [5], and abnormal signaling transduction pathways [6–8]. However, none of these possible mechanisms has been proven, and no universally accepted approach has been found to prevent the development of DN. The best therapeutic option is to arrest the development of DN at the earliest stage possible.

Mitofusin 2 (Mfn2, MGI:2442230) is a newly discovered multifunctional protein widely expressed in heart, skeletal muscle, liver, brain, kidney, and other organs [9, 10]. Mfn2 is essentially a transmembrane GTPase embedded in the mitochondrial outer membrane that mediates mitochondrial fusion [11]. Mfn2 deficiency and subsequent disruption of mitochondrial dynamics have been linked to

human neurodegenerative diseases, such as Charcot–Marie–Tooth type 2A, Parkinson's disease, and Alzheimer's disease [12, 13]. The physiologic and pathologic functions of Mfn2 are believed to extend beyond mitochondrial fusion. Emerging evidence indicates that Mfn2 inhibits the proliferation of various cells, including vascular smooth muscle cells and myocardial cells, and prevents neointimal hyperplasia [9, 14–16]. These effects of Mfn2 might be attributed to its influence on associated signaling pathways because it contains a characteristic amino acid sequence (N-DVKGYLSKVRGISEVL-C) that may act as a binding site for Ras, an upstream activator of the MAPK cascade [15–19].

Studies on the relationship between Mfn2 and diabetes are limited. Previous studies have found deficient mitochondrial oxidative phosphorylation and decreased Mfn2 expression in patients with type 2 diabetes and obesity [20–22], whereas exercise and weight loss increased Mfn2 expression [21, 23, 24]. In diabetic patients, insulin improves the mitochondrial structure [25]. Moreover, insulin influences the biogenesis of mitochondria by upregulating Mfn2, which may in turn block MEK-dependent signaling and activate the PI3K-signaling pathway [26]. These findings suggest that Mfn2 may participate in the pathogenesis of diabetes. However, studies investigating the function of Mfn2 in the kidneys are limited.

The morphology of mitochondria is determined by the balance between fission and fusion [27–29]. In the study by Brook, knockout of Bak (a Bcl-2 family protein) reduces cytochrome c release and apoptosis in transformed baby mouse kidney cells. The dissociation of Bak from Mfn2 may decrease mitochondrial fusion, thereby inducing mitochondrial fragmentation [30, 31]. Mitochondrial fragmentation has also been demonstrated in ischemic and in nephrotoxic models of acute renal failure. Mitochondrial fragmentation occurs early in many cytotoxic processes and contributes to the subsequent development of mitochondrial membrane permeabilization, release of apoptogenic factors, and cell apoptosis [32, 33]. These studies focused on the balance between mitochondrial fusion and fragmentation. However, other putative functions of Mfn2, such as regulation of signal transduction, have not been addressed.

As reported in previous studies, Mfn2 plays a protective role against cell injury; however, whether Mfn2 has similar protective effects in DN is unknown. Hence, the underlying mechanisms need to be addressed to exploit Mfn2 in clinical practice. Consequently, the primary objective of the present study is to investigate whether Mfn2 plays a protective role in the early stage of DN by evaluating the pathologic changes in the kidneys and the related molecular biological parameters in Mfn2-overexpressing diabetic rats (established by STZ injection). The second objective is to explore the possible mechanisms of Mfn2-mediated protection. Previous studies revealed that ECM accumulation in DN is closely associated with activation of the p38 MAPK-signaling pathway, oxidative stress, and mitochondrial dysfunction [34–39]. Therefore, we also examined oxidative stress parameters, mitochondrial function, and the changes in the p38 MAPK-signaling pathway during DN. To the best of our knowledge, this is the first study to investigate the role of Mfn2 in DN.

Materials and methods

Experimental animals

Male Sprague-Dawley rats (10 weeks old, weighing 200–250 g) were purchased from the Experimental Animal Center of Sichuan University. The rats were divided randomly into four groups of 32: an animal model group (group B) that received a single intraperitoneal injection of streptozotocin (STZ; 65 mg/kg) dissolved in citrate solution (0.1 M citric acid and 0.2 M sodium phosphate, pH 4.5), a control group (group A) that received an equivalent volume of citrate buffer alone, a Model + AdGFP group (group C), and a Model + AdMfn2 group (group D) that received injection of STZ at 7 days after adenovirus-mediated gene transfer in vivo. All animals injected with STZ developed diabetes, as indicated by plasma glucose levels >13.9 mmol/l at 48 h following the injection [40, 41]. All rats were fed the same diet and water. Insulin was not given to any of the animals. Blood and urine samples were collected and tested for glucose, urine protein, and urinary albumin/creatinine ratio. The rats were sacrificed to obtain the kidney tissue at the 0th, 2th, 4th, and 8th week(s) after STZ. The endpoint was set at the 8th week. Kidney and body weight were also measured. The study was conducted following the Principles of Laboratory Animal Care (NIH publication no. 85-23, revised in 1996) for the care and use of animals, and the protocol was approved by the Animal Care Committee of West China Hospital, Sichuan University, China.

Gene transfer

An adenovirus encoding the complete Mfn2 open reading frame (AdMfn2) and a control adenovirus encoding the green fluorescent protein open reading frame (AdGFP) were constructed by Vector Gene Technology Co., Ltd. A Vira Bind Adenovirus Purification Kit (Cell Biolabs) was used to multiply and purify viruses. The animals were anesthetized with intramuscular injection of ketamine (35 mg/kg) and xylazine (5 mg/kg). After median incision of the abdomen, the abdominal aorta below the renal vessels, inferior vena cava, and hepatic portal vessel were clamped. Approximately 3 ml of the adenoviral

vector-containing solution (either AdGFP or AdMfn2, titer at 1×10^{10} PFU/ml in 100 ml elution buffer plus 10% glycerol) was slowly injected into the renal artery through a cannula pre-implanted in the distal abdominal aorta. After 1 and 2 h, an additional 1 ml of adenovirus vector–containing solution was injected. After blood flow was re-established, the abdomen was closed, and the animals were allowed to recover. On the 7th day after gene transfer, Mfn2 expression was evaluated, and groups B, C, and D were injected with STZ [42].

Immunohistochemistry

Transfection efficiency was evaluated in the kidneys by immunohistochemical staining of 4-μm formalin-fixed, paraffin-embedded sections. Rabbit anti-mouse Mfn2 antibodies (1:1000 dilution, Sigma) were used as the primary antibodies. The sections were washed with PBS and incubated with biotinylated secondary antibody (donkey anti-rabbit IgG, 1:100 dilution; Jackson Immuno Research Labs) for 40 min. All the slides were counterstained with hematoxylin. The positively stained area of the renal glomerulus in each section was determined under a microscope. The positive staining area was calculated using Image-Pro Plus 6.0 image analytic system.

Real-time quantitative polymerase chain reaction

RNA was extracted from the kidney tissues using TRIzol reagent (Invitrogen) following the manufacturer's instructions. After DNase treatment (Promega), RNA was reverse transcribed into first strand cDNA using RevertAid™ First Strand cDNA Synthesis Kit (MBI). Cycling and real-time PCR detection were performed using an ABI PRISM® 7900 Sequence Detection System. Cycling conditions were as follows: 50°C for 2 min then 95°C for 10 min, followed by 35 cycles of 95°C for 30 s, 50°C for 45 s, and 72°C for 30 s. Gene-specific primers were designed using Vector NTI (Invitrogen), and expression of β-actin was used as the internal control for normalization. The primer pairs for Mfn2 amplification were 5′-ATGATAGACGGCTTG AA-3′ (F) and 5′-CGACTCCCTCTTTGTGA-3′(R), and the primers were 5′-CTTAGTTGCGTTACACCCTTTC-3′ (F) and 5′-CACCTTCACCGTTCCAGTTT-3′ (R) for β-actin. Transcription abundance was expressed as fold increase over the control gene calculated by the $2^{-\Delta\Delta Ct}$ method.

Histological analysis

Formalin-fixed, paraffin-embedded sections (4 μm) were stained with hematoxylin and eosin and Periodic acid-Schiff for light microscopic observation. Five glomeruli from each section were randomly selected to determine the average glomerular cross-sectional area (GA) under light microscopy using MIAS-2000 image analysis system (Zhisheng). The glomerular volume (GV) was calculated according to the following formula: $GV = \beta/k \times (GA)^{3/2}$, where $\beta = 1.38$ is a shape coefficient, and $k = 1.1$ is a size distribution coefficient [43]. The kidney tissues were treated for electron microscopy as previously described [44]. Ultrathin sections were cut, collected on cellodin-coated single slot grids, and stained with uranyl acetate and lead citrate. Digital images were obtained using a Leo906 transmission electron microscope. The average GBM thickness (GBMT) was measured from electron micrographs.

TdT-mediated dUTP nick end labeling (TUNEL) assay

The paraffin-embedded specimens were cut into 3-μm sections. Staining was performed using an in situ cell-death detection kit AP (Roche) according to the manufacturer's instructions. In brief, the tissue sections were treated with 20 μg/ml proteinase K for 30 min, washed with phosphate-buffered saline solution, and incubated with fluorescein-labeled nucleotides and terminal deoxynucleotidyl transferase for 60 min. The sections were then incubated with converter alkaline phosphatase for 30 min. The reaction was developed with Fast Red tablets in naphthol phosphate substrate (Laboratory Vision). Ten villi and crypts in each section were observed under fluorescence microscopy, and the average number of apoptotic cells per 100 counted cells was defined as the apoptotic index (AI).

Determination of ROS production in kidney tissue

Rat kidney homogenate was analyzed fluorometrically by measuring the oxidation of the non-fluorescent probe 20,70-dichloro-fluoresceindiacetate (DCFDA) into the fluorescent metabolites dichlorofluorescein (DCF) as described previously [45]. In brief, 30 ml of kidney homogenate in PBS was mixed with 5 μM DCF-DA and incubated for 30 min at room temperature. The mean fluorescence intensity was directly measured at excitation and emission wavelengths of 485 and 535 nm, respectively.

Determination of acetyl-CoA in isolated mitochondria

Mitochondria were isolated from rat kidney homogenates followed by multiple centrifugations at $700\times g$, $7800\times g$, and $10000\times g$ in ice-cold isolation buffer containing 50 mM Tris/HCl, pH 7.4, 250 mM sucrose, 5 mM EDTA, and protease inhibitors [46]. The mitochondrial protein concentration was determined by Bradford protein assay [47]. Free acetyl-CoA was determined in isolated mitochondria using high-performance liquid chromatography

(HPLC) as previously described [48]. Separation of acetyl-CoA was performed using an ODS-Hypersil column (Supelco SA). The UV detector was operated at 254 nm and set at 0.05 sensitivity. A mobile phase of 220 mM potassium phosphate containing 0.05% dithioglycol (solution A) and 98% methanol and 2% chloroform (solution B) was used. The flow rate was 0.4 ml/min, and the gradient was adjusted as previously described.

Western blot analysis

Kidney tissue was homogenized in ice-cold modified RIPA buffer [150 mM NaCl, 1% (v/v) Nonidet P-40, 0.25% (w/v) deoxycholate, 1 mM EDTA, and 50 mM Tris, pH 7.4] (Sigma). The protein concentration was determined using the Bradford assay (BioRad). Equal amounts of protein per lane from each sample was separated on 10% sodium dodecyl sulfate polyacylamide gels and transferred onto polyvinylidene fluoride membranes (Invitrogen). The membranes were probed overnight using the following antibodies: anti-Mfn2 (1:1000 dilution, Sigma), anti-phospho-p38 MAPK (1:2000 dilution, Santa Cruz), anti-p38 MAPK (1:2000 dilution, Santa Cruz), and anti-collagen IV (1:1000 dilution, Sigma). The immunolabeled membranes were incubated with a goat anti-rabbit IgG secondary antibodies (1:10000 dilution, Santa Cruz) for 0.5 h. The bands were visualized by enhanced chemiluminescence (Santa Cruz) and quantified by Quantity One software (Biorad). Sample loading was normalized by immunoblotting with an anti-β-actin monoclonal antibody (1:2000 dilution, Chemicon).

Statistical analyses

All values are expressed as means ± SEM. Multiple group means were compared by one-way ANOVA. The before and after within-group means were statistically evaluated using t tests. A value of $P < 0.05$ was considered statistically significant. The SPSS 11.5 statistical software was used for analysis.

Results

General findings

Three days after STZ injection, blood glucose reached the standard for diabetic models, and they were maintained at this high level from the 4th week to the 8th week. Comparison of the STZ-treated group B with groups C and D, which were subjected to STZ and adenovirus-mediated infection, indicates that the transfection protocol did not affect blood glucose concentration.

The kidney weight/body weight (KW/BW) of group B (STZ group) and group C (STZ + adenovirus expressing green fluorescent protein, AdGFP) rose significantly by the 4th week, whereas the KW/BW of group D (STZ + adenovirus expressing Mfn2, AdMfn2) was not significantly different from the untreated group A ($P > 0.05$). At the 8th week, the KW/BW of group D increased relative to group A, but was still significantly lower than that in group C ($P < 0.05$). Hence, the Mfn2 overexpression prevents pathologic kidney hypertrophy.

From the 2th week after modeling (STZ injection), proteinuria began to increase in rats of groups B and C, whereas proteinuria of group D was not significantly different from group A ($P > 0.05$). From the 4th and the 8th weeks onward, groups B and C exhibited even higher proteinuria, whereas the proteinuria in group D was still lower than group C.

At the 2th week after STZ injection, the urinary albumin/creatinine ratio (ACR) of groups B and C rose, whereas the ACR of group D did not increase until the 4th week. The ACR level was still lower than in group C. Thus, adenovirus-mediated Mfn2 overexpression, but not adenovirus-mediated GFP transfection, reduced several pathologic aspects of DN (data shown in Table 1).

Detection of gene transfection

The transfection efficiency as detected by real-time PCR method reached 70% (data not shown). Mfn 2 expression reached a peak in the 1st week after transfection and began to decay gradually from the 3rd week to the 9th week. However, it was still higher than the baseline ($P < 0.05$) until the 11th week when gene expression in the transfected animals was not significantly different from expression before transfection ($P > 0.05$) (Fig. 1I). A week after transfection, immunohistochemistry was also performed to detect the expression of Mfn2 in the kidneys. The amount of Mfn2 expression was digitally quantified using Image-Pro Plus 6.0. The positive staining area (%) in group D rats was significantly higher than in groups A and C ($P < 0.01$), whereas no difference was observed between the control group and group C (Fig. 1II, III).

Mfn2 protein expression over time

To test how Mfn2 expression changed with time, western blot analysis was performed on the kidney lysates prepared immediately after transfection and at the 2th, 4th, and 8th week(s). In groups B and C, Mfn2 expression was inhibited from the 2th week and the degree of inhibition increased with time, reaching a nadir by the 4th week. In the animals transfected with AdMfn2, Mfn2 protein expression decreased with time (Fig. 2) consistent with the RT-PCR results.

Table 1 General findings

	Group A	Group B	Group C	Group D
Glucose (mmol/l)				
0 week	7.13 ± 1.87	14.56 ± 1.23*	14.87 ± 1.56*	15.01 ± 1.92*
2 week	7.09 ± 1.12	27.37 ± 2.57*	26.72 ± 3.32*	26.53 ± 4.13*
4 week	7.32 ± 1.13	31.79 ± 3.67*	30.33 ± 4.01*	32.57 ± 3.23*
8 week	7.97 ± 1.01	29.91 ± 4.25*	30.12 ± 2.75*	30.56 ± 3.11*
KW/BW (mg/g × 10^3)				
0 week	3.87 ± 0.11	3.74 ± 0.21	3.9 ± 0.19	3.73 ± 0.25
2 week	3.69 ± 0.17	3.89 ± 0.34	3.94 ± 0.37	3.81 ± 0.45
4 week	3.91 ± 0.21	4.13 ± 0.45*	4.22 ± 0.51*	3.93 ± 0.63
8 week	3.94 ± 0.19	4.95 ± 0.62*	4.87 ± 0.49*	4.12 ± 0.55*#
Urine protein (mg/24 h)				
0 week	7.22 ± 3.32	7.53 ± 2.45	7.97 ± 3.11	7.14 ± 2.93
2 week	6.97 ± 2.67	10.32 ± 4.42*	11.23 ± 4.19*	8.24 ± 5.03#
4 week	8.14 ± 2.03	19.79 ± 5.65*	20.65 ± 6.31*	13.31 ± 3.29*#
8 week	7.32 ± 3.01	34.23 ± 6.87*	32.31 ± 4.29*	18.93 ± 3.65*#
ACR (mg/mmol)				
0 week	1.17 ± 0.18	1.32 ± 0.32	1.25 ± 0.23	1.10 ± 0.17
2 week	1.33 ± 0.57	2.45 ± 0.98*	2.67 ± 1.01*	1.67 ± 0.87
4 week	1.39 ± 0.33	3.72 ± 0.76*	3.91 ± 1.1*	1.95 ± 0.96*#
8 week	1.43 ± 0.69	5.35 ± 0.84*	5.89 ± 1.23*	2.95 ± 1.12*#

* Compared with the group A, $P < 0.05$

Compared with the group C, $P < 0.05$

Pathological analysis

The pathologic changes were not obvious within the first 4 weeks of treatment. However, the rats in groups B and C exhibited mesangial expansion, mesangial cell proliferation, and glomerular hypertrophy by the 8th week (Fig. 3I). The glomerular volume increased significantly in group C and was significantly higher than those of the rats in group D with Mfn2 overexpression (Fig. 3III). Glycogen content was also significantly different between groups C and D, as revealed by PAS (Fig. 3II). The GBM was thicker among the rats in groups B and C and was accompanied by fusion of podocytes. These changes were significantly less common in the group D rats (Fig. 3IV). The GBMT increased with time in group C and was markedly thicker than in the group D rats by the 8th week (Fig. 3V).

Expression of Collagen IV and phospho-p38 protein

Collagen IV is a main component of the ECM, and the expression of this protein can reflect the degree of renal damage. Western blot analysis shows that collagen IV expression significantly increased in groups B and C by the 8th week, whereas collagen IV expression in group D was statistically lower than in group C ($P < 0.05$) (Fig. 4I). Phospho-p38, the upstream activator of p38 MAPK, exhibited a similar trend, with lower levels in group D than in group C ($P < 0.05$) (Fig. 4II).

ROS production in kidney tissue, acetyl-coenzyme A in mitochondria, and mitochondrial morphologic measurements

ROS production was measured to determine the capacity of Mfn2 to alter the oxidative stress status of diabetic rat kidneys. As shown in Fig. 4III, the level of oxidation products rose significantly in groups B and C by the 8th week. On the other hand, Mfn2 overexpression inhibited oxidative stress. The expression of acetyl coenzyme A, a key protein in mitochondrial oxidative phosphorylation, was examined. Figure 4IV presents the acetyl coenzyme A contents of the kidneys in the different treatment groups. Acetyl coenzyme A increased in groups B and C concomitant with the rise of ROS, whereas Mfn2 overexpression decreased acetyl coenzyme A in mitochondria.

Electron microscopy revealed that the mitochondria of the proximal tubule cells showed conspicuous spherical enlargements in all the STZ-treated groups (Fig. 4V), and the mitochondrial matrix was more electrolucent than in the control rats. However, the mitochondrial membranes

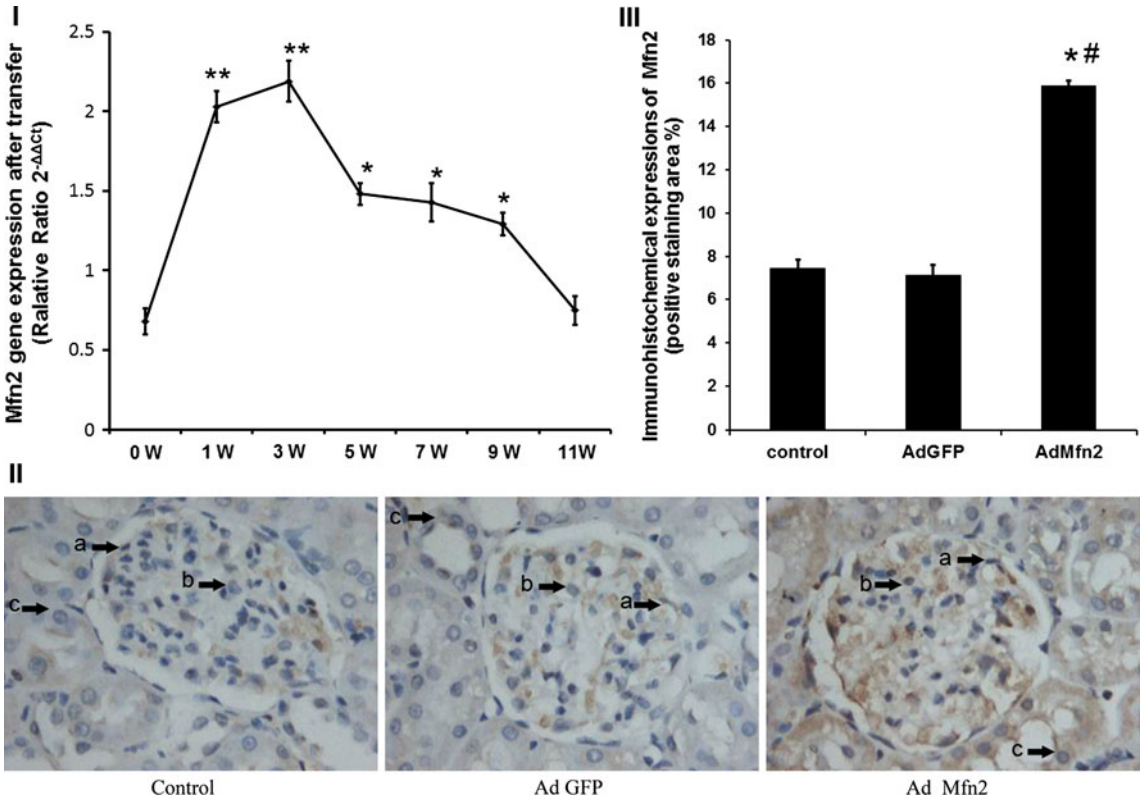

Fig. 1 Overexpression of Mfn2. I—Mfn2 gene expression with time was detected by realtime-PCR method (*$P < 0.05$, **$P < 0.01$, when compared with 0 week). II—Mfn2 expression in kidney tissues was detected by immunohistochemistry. On the 7th day after Mfn2 transfection, positive staining particles in glomeruli and tubules significantly increased. *Arrows*: *a* endothelium cells; *b* mesangial cells; *c* tubular epithelial cells. III—Quantitative image analysis showed that expression rate in AdMfn2 group was significantly higher than in the control group and the AdGFP group (*$P < 0.05$, when compared with control group; #$P < 0.05$, when compared with AdGFP group)

were well preserved in each group. Morphologic changes were less obvious in group D rats compared with those in group C.

Apoptosis

The TUNEL method was used to identify apoptotic cells in the diabetic rat kidneys. Few apoptotic cells were observed in the glomeruli, and renal tubular cells appeared to be the major apoptotic cells in the STZ-treated rats. The numbers of apoptotic cell were counted on the 8th week, and these counts revealed no significant difference in apoptosis index between groups ($P > 0.05$) (Fig. 5).

Discussion

Mounting evidence indicates that Mfn2 is a multifunctional protein with a biological function beyond regulation of mitochondrial shape. These additional functions of Mfn2 are now attracting closer attention, including regulation of mitochondrial metabolism, roles in multiple signaling pathways, regulation of apoptosis, determination of organelle shape, and regulation of cell cycle progression [9, 20, 21, 49, 50]. Few reports, if any, have examined the role of Mfn2 in diabetes and associated pathologies. Previous studies have indicated that Mfn2 expression is reduced in obesity and type 2 diabetes. The concomitant decrease in mitochondrial size suggests that Mfn2 plays some role in the etiology of insulin resistance. A positive correlation between Mfn2 levels and insulin sensitivity has been observed in morbidly obese subjects and after bariatric surgery [22, 24]. Based on these findings, Mfn2 presumably acts as an important factor in the pathogenesis of diabetes.

Research on the role of Mfn2 in DN has been limited. The effects of Mfn2 on diabetic kidneys at the earliest stages of DN remain undetermined. Our data demonstrate that endogenous Mfn2 expression is significantly inhibited in diabetic rats. Similarly, Bach et al. report that the expression of Mfn2 decreases in diabetic patients [22]. Considering that high glucose influences gene expression by regulating transcription factors [51, 52], hyperglycemia may inhibit Mfn2 expression. However, experimental confirmation is needed.

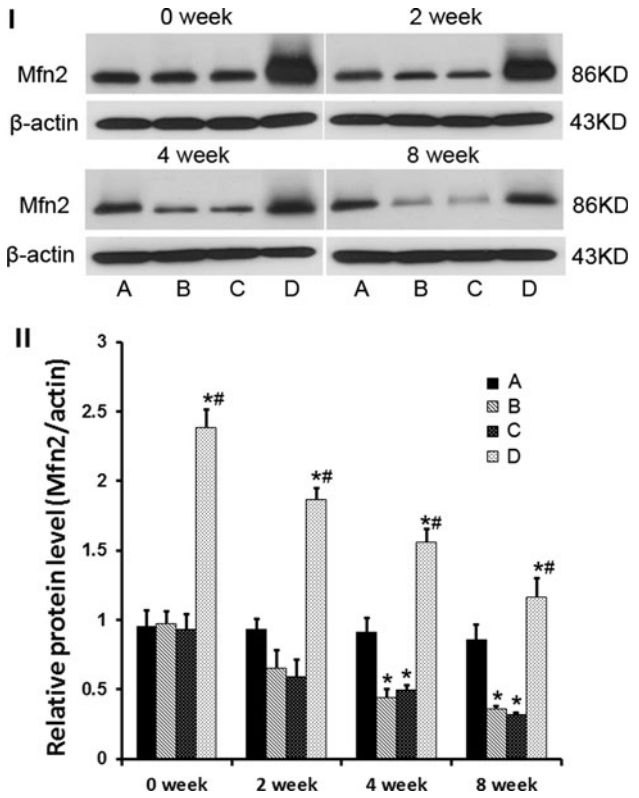

Fig. 2 Protein expression of Mfn2 with time. I—Protein expression of Mfn2 with time (0, 2th, 4th, and 8th weeks) in kidney tissues among the four groups detected by western blot. II—Relative quantity of Mfn2 expression level at different time points (*$P < 0.05$, when compared with group *A*; #$P < 0.05$, when compared with group *C*)

Clinical parameters indicative of DN were markedly ameliorated by virus-mediated Mfn2 overexpression. Indeed, Mfn2 overexpression is associated with decreased kidney volume (as indicated by KW/BW) and reduced proteinuria and ACR in diabetic rats, which indicate that Mfn2 slows the progression of DN. Light and electron microscopy reveal that Mfn2 overexpression limits mesangial expansion, glycogen accumulation, glomeruli enlargement, and thickening of the GBM, all being the hallmarks of diabetic kidney. Mfn2 overexpression also inhibits the synthesis of collagen IV, the main component of the ECM. However, the potential mechanism of the protective effect of Mfn2 remains unclear.

Brook et al. studied the effects of Mfn2 in cisplatin-induced acute tubular necrosis and found that Mfn2 had a protective influence on the kidney by inhibiting excessive apoptosis of renal tubular epithelial cells [30]. The extent of apoptosis was detected to investigate whether the protective role of Mfn2 in DN is associated with the regulation of apoptosis. However, no significant differences in the number of apoptotic cells (TUNEL+) was observed in any the rat group at the 8th week after the diabetic state was established. This phenomenon can be explained by the following: Apoptosis is not the major pathologic change in early stage DN. Therefore, the effect of mfn2 overexpression on apoptosis was not prominent [53, 54]. Diabetes is accompanied by the increased generation of ROS in several tissues, including the kidneys. Oxidative stress has emerged as a critical pathogenic process in the development of DN [55–58]. Hence, the correlations among Mfn2, oxidative stress, and mitochondrial function were examined. Previous studies have demonstrated that Mfn2 repression leads to a decrease in the oxidation of glucose, pyruvate, and palmitate, and to reduced mitochondrial membrane potential in myotubes. Conversely, Mfn2 overexpression in HeLa cells causes the perinuclear aggregation of mitochondria, a marked enhancement of mitochondrial membrane potential, and increased glucose oxidation [20, 21]. In the present study, ROS production in the DN rats increased slightly by the 8th week, accompanied by enhanced oxidative metabolism by the mitochondria. These signs of oxidative stress were ameliorated by Mfn2 overexpression. How Mfn2 influences mitochondrial ROS generation is still unknown. Hence, the influence of Mfn2 on ROS and mitochondrial function may have contributed to the partial protection against the development of DN. Further study is required to determine if this is caused by a direct antioxidant effect. Mitochondrial enlargement was observed following STZ injection. However, these mitochondrial changes are not solely attributable to diabetes because STZ has direct deleterious effects on the kidneys [59] and it can cause morphologic changes in the mitochondria. In the present study, Mfn2 overexpression improved some mitochondrial functions without decreasing glucose, which may be explained by the local Mfn2 transfection. Skeletal muscles and adipose tissues, rather than the kidneys, are responsible for glucose regulation.

Recent studies have confirmed the significant anti-proliferation effect of Mfn2. Mfn2 inhibits the proliferation of vascular smooth muscle cells and hepatocellular carcinoma cells [60]. Mfn2 interact with RAS [19], which suggests a potential role in regulating Ras-dependent MAPK signaling. Mounting evidence has implicated p38 MAPK signaling in the development of DN [5, 61]. High glucose has been demonstrated to promote p38 MAPK activation and collagen IV production in podocytes [62, 63]. Again, the present study confirmed that p38 activation induces collagen synthesis, whereas collagen synthesis is depressed when p38 is inactivated. Mfn2 overexpression significantly inhibits p38 activation. Therefore, we hypothesize that Mfn2 directly inhibits the p38 MAPK pathway through p38 dephosphorylation, further decreasing collagen synthesis. This mechanism might account for the protective role of Mfn2 in DN.

To the best of our knowledge, the present study is the first to link Mfn2 to diabetic kidney disease. The experimental results are optimistic, but the potential role of Mfn2

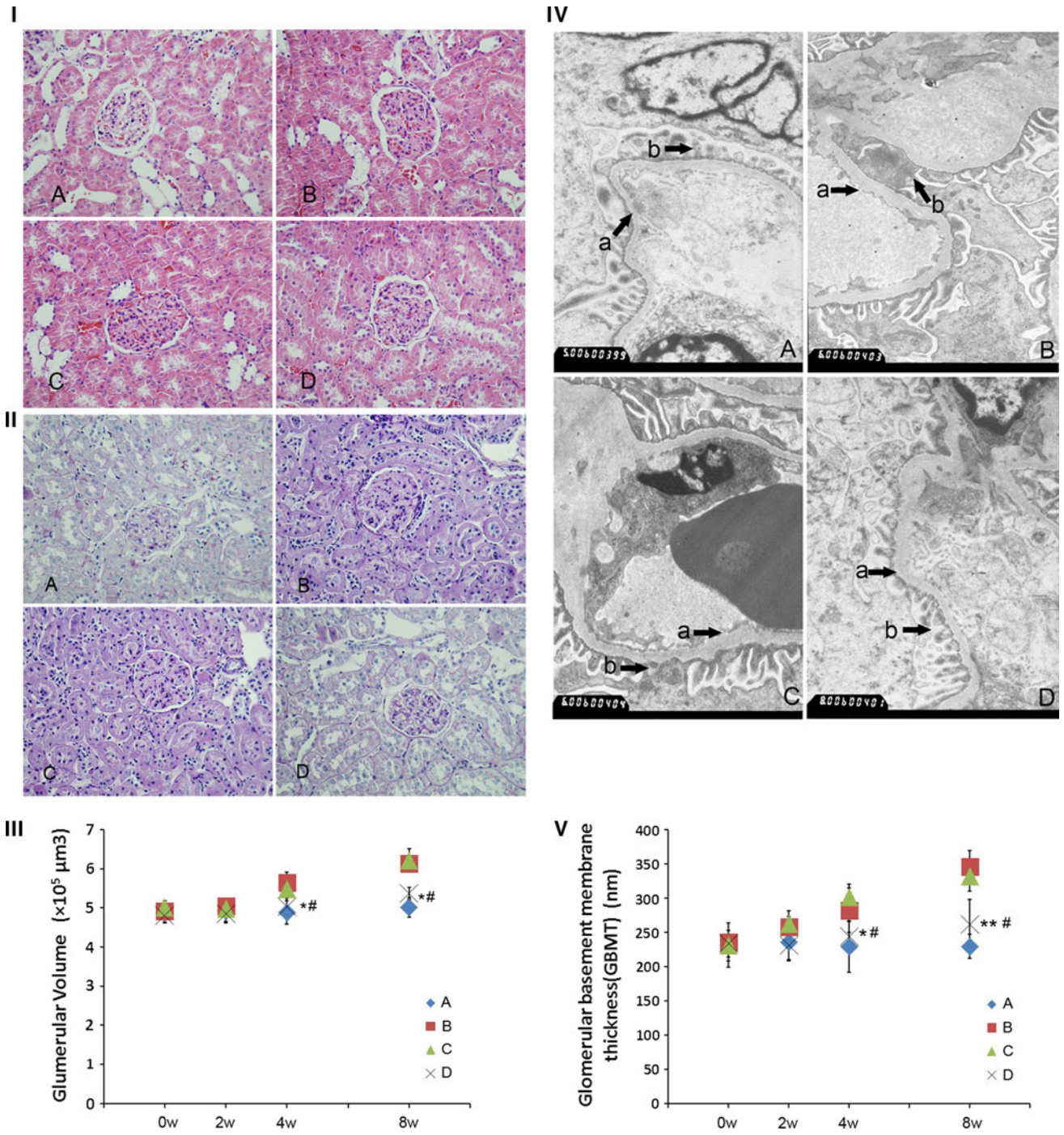

Fig. 3 Pathological changes of kidney in STZ-induced diabetic rat. Renal tissue morphology was significantly improved by overexpression of Mfn2 in the 8th week. I—HE staining revealed manifestations of early DN in groups *B* and *C*, including enlargement of glomeruli and mesangial expansion; while the changes were less obvious in group *D*. II—PAS staining showed increase of glycogen in glomeruli in groups *B* and *C*; while the changes were less obvious in group *D*. III—GV at different time points in each group revealed some differences in the 4th week. IV—GBM changes in the 8th week were observed by electron microscopy. Basement membrane thickness and foot process fusion can be seen in the groups *B* and *C*, whereas the group *D* had relatively minor changes with normal basement membrane and foot process arranged in order. *Arrows*: *a* GBM; *b* foot process. V—GBMT at different time points in each group showed some changes in the 4th week. The group *D* had relatively minor changes (*$P < 0.05$, compared with the group *C*; **$P < 0.01$, compared with the group *C*; #$P < 0.05$ compared with the group *A*)

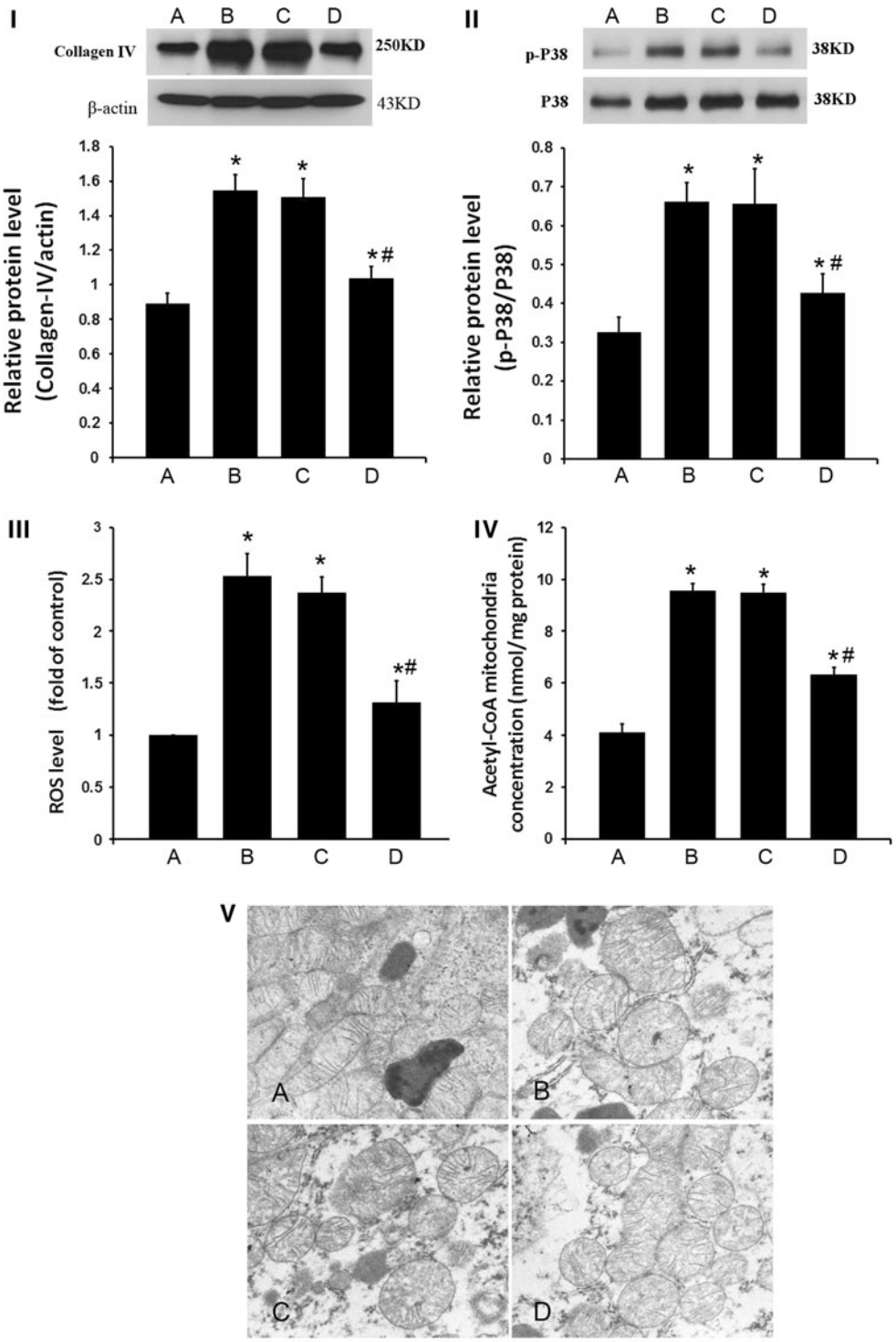

Fig. 4 Related protein expression, ROS production and mitochondrial measurement. Overexpression of Mfn2 significantly inhibited collagen synthesis, decreased the expression of phosphor-p38 and ROS production, and regulated mitochondrial function (*$P < 0.05$, compared with the group *A*; #$P < 0.05$, compared with the group *C*). I—Protein expression of collagen IV (western blot). II—Protein expression of phospho-p38 and p38 (western blot). III—ROS production in kidney tissue (DCF method). IV—Free acetyl-CoA in isolated mitochondria (HPLC method). V—Mitochondria in proximal tubule cells diffusely enlarged in the groups *B*, *C*, and *D*, as compared with the group *A*. The change of mitochondrial morphology was less obvious in group *D* than in group *C*. Both ×12,000

in the development and progression of diabetic kidney disease remains largely unexplored. Mfn2 regulates ROS production through the mitochondria and influences p38 MAPK-signaling pathway, whereas p38 is directly activated by ROS [64]. The association of Mfn2, ROS, and p38 MAPK might be the key to understanding the role of Mfn2 in DN.

The present study has some limitations. Evidence to confirm a direct interaction between Mfn2 and Ras or between Mfn2 and kidney mitochondria has not been found. Second, Mfn2 expression after transfection in vivo gradually decayed over time, whereas DN develops slowly. The development of Mfn2 transgenic animals or Mfn2 knockout animals will allow further extension of the present study.

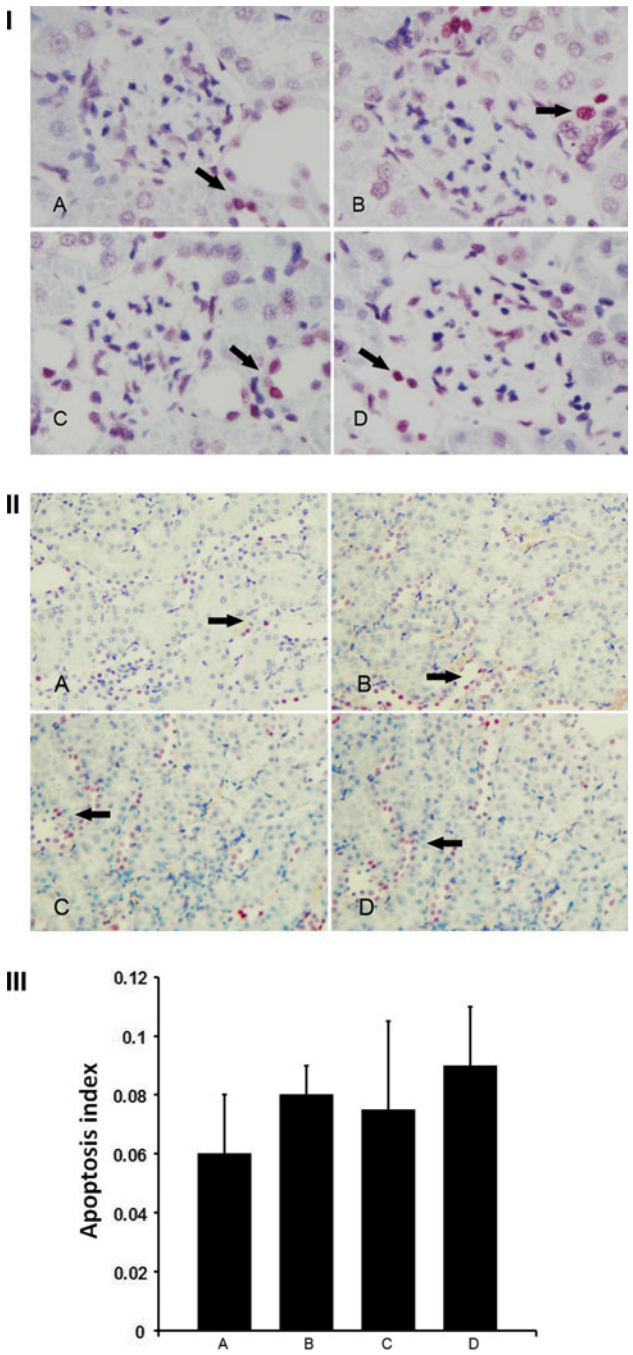

Fig. 5 Apoptosis in the diabetic kidney. I—The diabetic kidney apoptosis stain in glomerular (TUNEL method). *Arrows*: apoptosis cells. II—The diabetic kidney apoptosis stain in tubules. (TUNEL method). *Arrows* apoptosis cells. III—Apoptosis index. There were no significant differences among these groups at the 8th week ($P > 0.05$)

In summary, Mfn2 overexpression attenuates many of the pathologic changes in kidney structure and function associated with diabetes in rats. Mfn2 plays a protective role in DN, possibly by ameliorating oxidative stress, sustaining mitochondrial function, or by suppressing the p38 MAPK-signaling pathway. Furthermore, Mfn2 is a potential therapeutic target for the treatment of early DN.

Acknowledgements The authors thank Dr. Wu HT for technical assistance.

Conflicts of interest None.

References

1. Y. Qian, E. Feldman, S. Pennathur, M. Kretzler, F.C. Brosius, From fibrosis to sclerosis, mechanism of glomerulosclerosis in diabetic nephropathy. Diabetes **57**, 1439–1455 (2008)
2. A.Y. Lee, S.K. Chung, S.S. Chung, Demonstration that polyol accumulation is responsible for diabetic cataract by the use of transgenic mice expressing the aldose reductase gene in the lens. Proc. Natl. Acad. Sci. **92**, 2780–2784 (1995)
3. D. Koya, G.L. King, Protein kinase C activation and the development of diabetic complications. Diabetes **47**, 859–866 (1998)
4. D. Aronson, Potential role of advanced glycosylation end products in promoting restenosis in diabetes and renal failure. Med. Hypotheses **59**, 297–301 (2002)
5. M. Brownlee, Biochemistry and molecular cell biology of diabetic complications. Nature **414**, 813–820 (2001)
6. M.H. De Borst, J. Prakash, W.B. Melenhorst, M.C. van den Heuvel, R.J. Kok, G. Navis, H. van Goor, Glomerular and tubular induction of the transcription factor c-Jun in human renal disease. J. Pathol. **213**, 219–222 (2007)
7. A.B. el-Remessy, M. Bartoli, D.H. Platt, D. Fulton, R.B. Caldwell, Oxidative stress inactivates VEGF survival signaling in retinal endothelial cells via PI 3-kinase tyrosine nitration. J. Cell Sci. **118**, 243–252 (2005)
8. H. Fujita, S. Omori, K. Ishikura, M. Hida, M. Awazu, ERK and p38 mediate high-glucose-induced hypertrophy and TGF-β expression in renal tubular cells. Am. J. Physiol. Renal Physiol. **286**, F120–F126 (2004)
9. C. Kuang-Hueih, G. Xiaomei, Ma. Dalong, G. Yanhong, L. Qian, Y. Dongmei, L. Pengfei, Q. Xiaoyan, W. Shaojun, X. Rui-Ping, T. Jian, Dysregulation of HSG triggers vascular proliferative disorders. Nat. Cell Biol. **6**, 872–883 (2004)
10. O.M. de Brito, L. Scorrano, A mitochondria-shaping protein with signaling roles beyond fusion. Antioxid. Redox. Signal. **10**, 621–633 (2008)
11. M. Neuspiel, R. Zunino, S. Gangaraju, P. Rippstein, H. McBride, Activated mitofusin 2 signals mitochondrial fusion, interferes with bax activation, and reduces susceptibility to radical induced depolarization. J. Biol. Chem. **280**, 25060–25070 (2005)
12. M. Liesa, M. Palacín, A. Zorzano, Mitochondrial dynamics in mammalian health and disease. Physiol. Rev. **89**, 799–845 (2009)
13. H. Chen, D.C. Chan, Mitochondrial dynamics—fusion, fission, movement, and mitophagy—in neurodegenerative diseases. Hum. Mol. Genet. **18**(R2), R169–R176 (2009)
14. A. Jahani-Asl, E.C. Cheung, M. Neuspiel, J.G. MacLaurin, A. Fortin, D.S. Park, H.M. McBride, R.S. Slack, Mitofusin 2 protects cerebellar granule neurons against injury-induced cell death. J. Biol. Chem. **282**, 23788–23798 (2007)
15. H. Yu, Y. Guo, L. Mi, X. Wang, L. Li, W. Gao, Mitofusin 2 inhibits angiotensin II-induced myocardial hypertrophy. J. Cardiovasc. Pharmacol. Ther. **16**, 205–211 (2011)
16. F. Lu, X.-L. Moore, X.-M. Gao, M. Dart Anthony, L. Yean Leng, X.-J. Du, Down-regulation of mitofusin2 expression in cardiac hypertrophy in vitro and in vivo. Life. Sci. **80**, 2154–2160 (2007)
17. S. Fritz, D. Rapaport, E. Klanner, W. Neupert, B. Westermann, Connection of the mitochondrial outer and innermembranes by Fzol is critical for organellarfusion. J. Cell Biol. **152**, 683–692 (2001)

18. W. Wang, X. Cheng, J. Lu, J. Wei, G. Fu, F. Zhu, C. Jia, L. Zhou, H. Xie, S. Zheng, Mitofusin-2 is a novel direct target of p53. Biochem. Biophys. Res. Commun. **400**, 587–592 (2010)
19. O.M. de Brito, L. Scorrano, Mitofusin-2 regulates mitochondrial and endoplasmic reticulum morphology and tethering, the role of Ras. Mitochondrion **9**, 222–226 (2009)
20. D. Bach, S. Pich, F.X. Soriano, N. Vega, B. Baumgartner, J. Oriola, J.R. Daugaard, J. Lloberas, M. Camps, J.R. Zierath, R. Rabasa-Lhoret, H. Wallberg-Henriksson, M. Laville, M. Palacin, H. Vidal, F. Rivera, M. Brand, A. Zorzano, Mitofusin-2 determines mitochondrial network architecture and mitochondrial metabolism, a novel regulatory mechanism altered in obesity. J. Biol. Chem. **278**, 17190–17197 (2003)
21. S. Pich, D. Bach, P. Briones, M. Liesa, M. Camps, X. Testar, M. Palacin, A. Zorzano, The Charcot-Marie-Tooth type 2A gene product, Mfn2, up-regulates fuel oxidation through expression of OXPHOS system. Hum. Mol. Genet. **14**, 1405–1415 (2005)
22. D. Bach, D. Naon, S. Pich, F.X. Soriano, N. Vega, J. Rieusset, M. Laville, C. Guillet, Y. Boirie, H. Wallberg-Henriksson, M. Manco, M. Calvani, M. Castagneto, M. Palacin, G. Mingrone, J.R. Zierath, H. Vidal, A. Zorzano, Expression of Mfn2, the Charcot-Marie-Tooth neuropathy type 2A gene, in human skeletal muscle, effects of type 2 diabetes, obesity, weight loss, and the regulatory role of tumor necrosis factor alpha and interleukin-6. Diabetes **54**, 2685–2693 (2005)
23. R. Cartoni, B. Leger, M.B. Hock, M. Praz, A. Crettenand, S. Pich, J.L. Ziltener, F. Luthi, O. Deriaz, A. Zorzano, C. Gobelet, A. Kralli, A.P. Russell, Mitofusins 1/2 and ERRalpha expression are increased in human skeletal muscle after physical exercise. J. Physiol. **567**, 349–358 (2005)
24. G. Mingrone, M. Manco, M. Calvani, M. Castagneto, D. Naon, A. Zorzano, Could the low level of expression of the gene en- coding skeletal muscle mitofusin-2 account for the metabolic inflexibility of obesity? Diabetologia **48**, 2108–2114 (2005)
25. I. Vanhorebeek, R. De Vos, D. Mesotten, P.J. Wouters, C. Wolf-Peeters, B.G. Van den, Protection of hepatocyte mitochondrial ultrastructure and function by strict blood glucose control with insulin in critically ill patients. Lancet **365**, 53–59 (2005)
26. P. Pawlikowska, B. Gajkowska, A. Orzechowski, Mitofusin 2 (Mfn2), a key player in insulin-dependent myogenesis in vitro. Cell Tissue Res. **327**, 571–581 (2007)
27. D.C. Chan, Mitochondrial fusion and fission in mammals. Annu. Rev. Cell. Dev. Biol. **22**, 79–99 (2006)
28. K. Okamoto, J.M. Shaw, Mitochondrial morphology and dynamics in yeast and multicellular eukaryotes. Annu. Rev. Genet. **39**, 503–536 (2005)
29. B. Westermann, Molecular machinery of mitochondrial fusion and fission. J. Biol. Chem. **283**, 13501–13505 (2008)
30. C. Brooks, Q. Wei, L. Feng, G. Dong, Y. Tao, L. Mei, Z.J. Xie, Z. Dong, Bak regulates mitochondrial morphology and pathology during apoptosis by interacting with mitofusins. Proc. Natl. Acad. Sci. USA **104**, 11649–11654 (2007)
31. C. Brooks, S. Cho, C. Wang, T. Yang, Z. Dong, Fragmented mitochondria are sensitized to Bax insertion and activation during apoptosis. Am. J. Physiol. Cell. Physiol. **300**, C447–C455 (2011)
32. C. Brooks, Q. Wei, S.G. Cho, Z. Dong, Regulation of mitochondrial dynamics in acute kidney injury in cell culture and rodent models. J. Clin. Invest. **119**, 1275–1285 (2009)
33. S. Wu, F. Zhou, Z. Zhang, D. Xing, Mitochondrial oxidative stress causes mitochondrial fragmentation via differential modulation of mitochondrial fission-fusion proteins. FEBS. J. **278**, 941–954 (2011)
34. G.H. Tesch, MCP-1/CCL2, a new diagnostic marker and therapeutic target for progressive renal injury in diabetic nephropathy. Am. J. Physiol. Renal Physiol. **294**, 697–701 (2008)
35. J. Dong-Sub, L. Jin Ji, K. Seung-Jae, L. Sun Ha, P. Jehyun, S. Young Soo, Y. Tae-Hyun, H. Seung Hyeok, L. Jung Eun, K. Dong Ki, M. Sung Jin, K. Yu Seun, H. Dae Suk, K. Shin-Wook, FR167653 inhibits fibronectin expression and apoptosis in diabetic glomeruli and in high-glucose-stimulated mesangial cells. Am. J. Physiol. Renal Physiol. **295**, 595–604 (2008)
36. B.Y. Chin, A. Mohsenin, S.X. Li, A.M. Choi, M.E. Choi, Stimulation of pro-alpha(1)(I) collagen by TGF-beta(1) in mesangial cells, role of the p38 MAPK pathway. Am. J. Physiol. Renal Physiol. **280**, 495–504 (2001)
37. L.S. Chaturvedi, S. Koul, A. Sekhon, A. Bhandari, M. Menon, H.K. Koul, Oxalate selectively activates p38 mitogen-activated protein kinase and c-Jun Nterminal.kinase signal transduction pathways in renal epithelial cells. J. Biol. Chem. **277**, 13321–13330 (2002)
38. A. Pozzi, R. Zent, S. Chetyrkin, C. Borza, N. Bulus, P. Chuang, D. Chen, B. Hudson, P. Voziyan, Modification of collagen IV by glucose or methylglyoxal alters distinct mesangial cell functions. J. Am. Soc. Nephrol. **20**, 2119–2125 (2009)
39. P.D. Ribaldo, D.S. Souza, S.K. Biswas, K. Block, J.M. Lopes de Faria, J.B. Lopes de Faria, Green tea (Camellia sinensis) attenuates nephropathy by downregulating Nox4 NADPH oxidase in diabetic spontaneously hypertensive rats. J. Nutr. **139**, 96–100 (2009)
40. T.N. Sato, Y. Tozawa, U. Deutsch, K. Wolburg Buchholz, Y. Fujiwara, M. Gendron Maguire, T. Gridley, H. Wolburg, W. Risau, Y. Qin, Distinct roles of the recept or tyrosin kinases Tie-1 and Tie-2 in blood vessel formation. Nature **376**, 70–74 (1995)
41. A. Inada, K. Nagar, H. Aiar, Establishment of a diabetic mouse model with progressive diabetic nephropathy. Am. J. Pathol. **167**, 327–336 (2005)
42. P. Moullier, G. Friedlander, D. Calise, P. Ronco, M. Perricaudet, N. Ferry, Adenoviral-mediated gene transfer to renal tubular cells in vivo. Kidney Int. **45**, 1220–1225 (1994)
43. Y. Yamamoto, Y. Maeshima, H. Kitayama, S. Kitamura, Y. Takazawa, H. Sugiyama, Y. Yamasaki, H. Makino, Tumstatin peptide, an inhibitor of angiogenesis, prevents glomerular hypertrophy in the early stage of diabetic nephropathy. Diabetes **53**, 1831–1840 (2004)
44. R. Cartoni, E. Arnaud, J.-J. Me'dard, O. Poirot, D.S. Courvoisier, R. Chrast, J.-C. Martinou, Expression of mitofusin 2R94Q in a transgenic mouse leads to Charcot–Marie–Tooth neuropathy type 2A. Brain **133**, 1460–1469 (2010)
45. E. Topo, G. Fisher, A. Sorricelli, F. Errico, A. Usiello, A. D'Aniello, Thyroid hormones and D-aspartic acid, D-aspartate oxidase, D-aspartate racemase, H2O2, And ROS in rats and mice. Chem. Biodivers. **7**, 1467–1478 (2010)
46. S.M. Bailey, K.K. Andringa, A. Landar, V.M. Darley-Usmar, Proteomic approaches to identify and characterize alterations to the mitochondrial proteome in alcoholic liver disease. Methods Mol. Biol. **447**, 369–380 (2008)
47. M.M. Bradford, A rapid and sensitive method for the quantitation of microgram quantities of protein utilizing the principle of protein–dye binding. Anal. Biochem. **72**, 248–254 (1976)
48. W. Lysiak, K. Lilly, F. DiLisa, P.P. Toth, L.L. Bieber, Quantitation of the effect of L-carnitine on the levels of acid-soluble short-chain acyl-CoA and CoASH in rat heart and liver mitochondria. J. Biol. Chem. **263**, 1151–1156 (1988)
49. R. Sugioka, S. Shimizu, Y. Tsujimoto, Fzo1, a protein involved in mitochondrial fusion, inhibits apoptosis. J. Biol. Chem. **279**, 52726–52734 (2004)
50. M. Schrader, Shared components of mitochondrial and peroxisomal division. Biochim. Biophys. Acta **1763**, 531–541 (2006)
51. T. Yu, J.L. Robotham, Y. Yoon, Increased production of reactive oxygen species in hyperglycemic conditions requires dynamic

change of mitochondrial morphology. Proc. Natl. Acad. Sci. USA **103**, 2653–2658 (2006)
52. F.R. Danesh, M.M. Sadeghi, N. Amro, C. Philips, L. Zeng, S. Lin, A. Sahai, Y.S. Kanwar, 3-Hydroxy-3-methylglutaryl CoA reductase inhibitors prevent high glucose-induced proliferation of mesangial cells via modulation of Rho GTPase/p21 signaling pathway, Implications for diabetic nephropathy. Proc. Natl. Acad. Sci. USA **99**, 8301–8305 (2002)
53. E. Riedl, F. Pfister, M. Braunagel, P. Brinkkötter, P. Sternik, M. Deinzer, S.J. Bakker, R.H. Henning, J. van den Born, B.K. Krämer, G. Navis, H.P. Hammes, B. Yard, H. Koeppel, Carnosine prevents apoptosis of glomerular cells and podocyte loss in STZ diabetic rats. Cell. Physiol. Biochem. **28**, 279–288 (2011)
54. E. Sohn, J. Kim, C.S. Kim, Y.S. Kim, D.S. Jang, J.S. Kim, Extract of the aerial parts of Aster koraiensis reduced development of diabetic nephropathy via anti-apoptosis of podocytes in streptozotocin-induced diabetic rats. Biochem. Biophys. Res. Commun. **391**, 733–738 (2010)
55. Y. Hinokio, S. Suzuki, M. Hirai, M. Chiba, A. Hirai, T. Toyota, Oxidative DNA damage in diabetes mellitus, its association with diabetic complications. Diabetologia **42**, 995–998 (1999)
56. C.G. Schnackenberg, Oxygen radicals in cardiovascular-renal disease. Curr. Opin. Pharmacol. **2**, 121–125 (2002)
57. M.L. Onozato, A. Tojo, A. Goto, T. Fujita, C.S. Wilcox, Oxidative stress and nitric oxide synthase in rat diabetic nephropathy, effects of ACEI and ARB. Kidney Int. **61**, 186–194 (2002)
58. D. Koya, K. Hayashi, M. Kitada, A. Kashiwagi, R. Kikkawa, M. Haneda, Effects of antioxidants in diabetes-induced oxidative stress in the glomeruli of diabetic rats. J. Am. Soc. Nephrol. **14**(Suppl. 3), 250–253 (2003)
59. K. Kavanagh, D.M. Flynn, C. Nelson, L. Zhang, J.D. Wagner, Characterization and validation of a streptozotocin-induced diabetes model in the vervet monkey. J. Pharmacol. Toxicol. Methods **63**, 296–303 (2011)
60. W. Wang, J. Lu, F. Zhu, J. Wei, C. Jia, Y. Zhang, L. Zhou, H. Xie, S. Zheng, Pro-apoptotic and anti-proliferative effects of mitofusin-2 via Bax signaling in hepatocellular carcinoma cells. Med Oncol A (2010). doi:10.1007/s12032-010-9779-6
61. E. Paine, R. Palmantier, S.K. Akiyama, K. Olden, J.D. Roberts, Arachidonic acid activates mitogen-activated protein (MAP) kinase-activated protein kinase 2 and mediates adhesion of a human breast carcinoma cell line to collagen type IV through a p38 MAP kinase-dependent pathway. J. Biol. Chem. **275**, 11284–11290 (2000)
62. M.A. Reddy, S.G. Adler, Y.-S. Kim, L. Lanting, J. Rossi, S.-W. Kang, J. Nadler, A. Shahed, R. Natarajan, Interaction between MAPK and 12-lipoxygenase pathways in mediating growth and matrix protein expression in rat mesangial cells. Am. J. Physiol. **283**, F985–F994 (2002)
63. S.W. Kang, R. Natarajan, A. Shahed, C.C. Nast, J. LaPage, P. Mundel, C. Kashtan, S.G. Adler, Role of 12-lipoxygenase in the stimulation of p38 mitogen-activated protein kinase and collagen alpha5(IV) in experimental diabetic nephropathy and in glucose-stimulated podocytes. J. Am. Soc. Nephrol. **14**, 3178–3187 (2003)
64. N.A. Calcutt, M.E. Cooper, T.S. Kern, A.M. Schmidt, Therapies for hyperglycaemia-induced diabetic complications, from animal models to clinical trials. Nat. Rev. Drug Discov. **8**, 417–429 (2009)